# Switched reluctance motors with segmental rotors

B.C. Mecrow, J.W. Finch, E.A. El-Kharashi and A.G. Jack

**Abstract:** The magnetic design of switched reluctance motors is examined and an alternative design presented in which the rotor is made from a series of discrete segments. Single-phase machines are initially examined and design rules established. Predictions of airgap force density are presented as a function of electric loading and compared with toothed rotor equivalents. It is shown that much greater force densities are theoretically possible with the segmental design. The authors then proceed to apply the concepts developed to a three-phase configuration, which shows particular advantages. Measured test results from a three-phase machine are presented and compared with a conventional switched reluctance motor of the same dimensions, revealing both the advantages and disadvantages of the segmental rotor configuration.

### List of principal symbols

| | |
|---|---|
| $A$ | electric loading in terms of RMS MMF per unit length of periphery |
| $F$ | force |
| $W'$ | co-energy |
| $l$ | axial length |
| $t$ | width of airgap which actively carries magnetic flux in the aligned position |
| $x$ | distance between adjacent rotor segments |
| $y$ | width of triangular stator slot closure at the airgap |
| $\phi$ | magnetic flux |
| $\lambda$ | slot pitch |

*Subscripts*

| | |
|---|---|
| r | referred to rotor |
| s | referred to stator. |

## 1 Introduction

The magnetic geometry of switched reluctance machines (SRMs) has been effectively fixed for over 20 years. The basic structure consists of a series of stator teeth or poles, magnetically connected together by a core back, and a series of rotor teeth, with the magnetic circuit completed by a rotor core back. The effect of the tooth width on torque production [1–5] and acoustic noise [6–8] is well established: the influence of pole number on mean torque ascertained [9], and designs which reduce torque ripple determined [10–12]. There has been examination of the optimum shape of tooth tip and whether the tooth should be tapered [5, 13]. Multi-tooth per pole designs have been studied [14–16], but not generally developed, so the geometry effectively remains fixed. Rotor and stator teeth are generally straight or only slightly tapered: the tooth width of both rotor and stator is typically 30–45% of the pole pitch and the tooth tips do not have substantial pole shoes.

There has been greater diversity in the electrical design of SRMs. The majority continue to use simple concentrated windings, wrapped around a single tooth, because of their simplicity and short end-windings. However, there have been developments using fully pitched windings to increase the electrical utilisation of the machine, thus improving torque capability [17, 18], at the expense of increased end-winding length. There has also been the introduction of additional 'commutating' windings [19], which seek to aid commutation between phases by storing the magnetic energy within the machine, rather than passing it back into the supply.

The above discussion should be contrasted with synchronous reluctance motors, where the magnetic design of their rotors has been extensively refined. Over 30 years ago a simple toothed rotor structure, as still used in switched reluctance machines, was shown to give relatively low torque, due to a small saliency ratio between the $d$ and $q$ axes. Improved performance was demonstrated with segmental rotor constructions [20, 21], later leading to flux-barrier designs [22, 23] and axially laminated designs [24, 25].

This paper will show how, with modification, some of the developments of synchronous reluctance motor magnetic design can be applied to SRMs. It will build on some early work in this area by Lipo and Xu [26–28], who built a two-phase axially laminated machine, along with a patent placed by Horst, concerning a two-phase segmental motor for unidirectional operation [29]. Note is also taken of the work of Davis [30, 31], which concluded that an axially laminated SRM rotor was not necessarily advantageous.

## 2 Fundamental magnetic design concepts

The machines considered in this work will be referred to as switched reluctance machines rather than synchronous reluctance machines. This is because the machine is excited with a series of pulsating excitation patterns rather than the smoothly rotating excitation pattern used in synchronous reluctance machines.



*IEE Proceedings* online no. 20020345

*DOI:* 10.1049/ip-epa:20020345

Paper first received 13th December 2001

The authors are with the Power Electronics, Drives and Machines Group, Department of Electrical and Electronic Engineering, The University of Newcastle Upon Tyne, NE1 7RU, UK

To reveal the fundamental points of the magnetic design the geometry is simplified as much as possible. For this reason a single-phase, rectilinear machine with an equal number of stator and rotor slots has been chosen. Fig. 1 shows the geometry and the minimal region which has been modelled using the finite element method. Note that the rotor and stator core backs have been modelled as infinitely permeable boundaries. The rotor and stator teeth are parallel sided and of equal width. Fig. 1 also shows the principal dimensions chosen for the comparison. A slot pitch, $\lambda$, of 20.0 mm is used, along with an airgap length of 0.3 mm. A standard silicon steel magnetisation curve is assumed for the magnetic components. The width of the teeth, $t$, is varied, whilst other dimensions are held fixed.

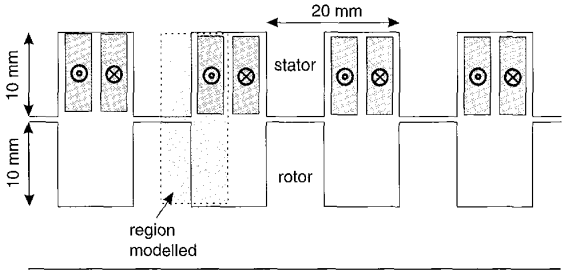


**Fig. 1** *Simple rectilinear model of a standard doubly salient toothed structure*

Fig. 2 shows the magnetic flux distribution for the aligned and unaligned positions, produced using a two dimensional finite element simulation. Rotor teeth are chosen to be deep, so that fringing to the rotor core back does not play a major part in the unaligned inductance.

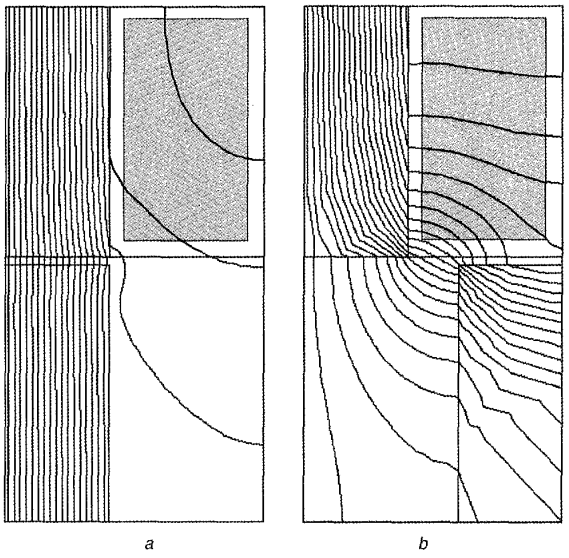


**Fig. 2** *Magnetic flux plots for a doubly salient toothed structure, exploiting symmetry around the tooth and slot centre line*
*a* Aligned position; *b* unaligned position

Fig. 3 shows the average flux linking each turn per unit axial length of the model as a function of the slot MMF. Six different values of the ratio tooth width to slot pitch, $t/\lambda$, are shown, varying from 0.3 to 0.8. As expected, both the

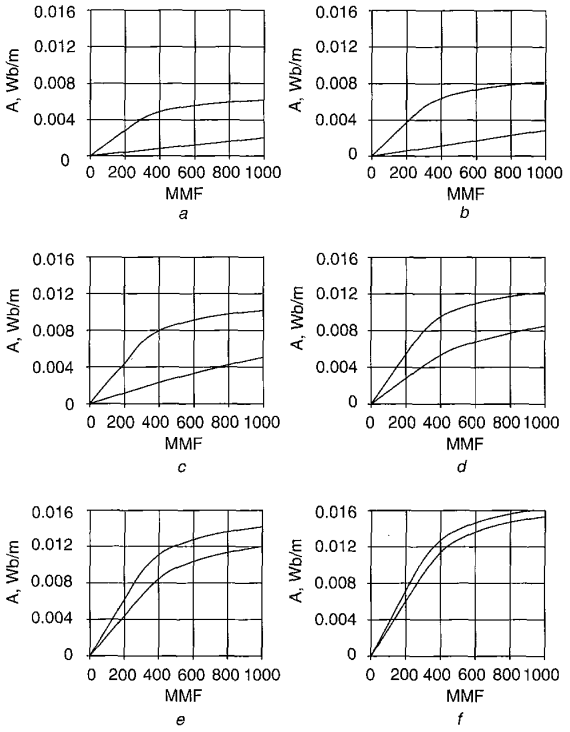


**Fig. 3** *Average magnetic vector potential against MMF per half-slot for a doubly salient toothed structure, showing variation with $t/\lambda$*
*$t/\lambda$: a* 0.30; *b* 0.40; *c* 0.50; *d* 0.60; *e* 0.70; *f* 0.80

aligned and unaligned flux linkage rises with tooth width. Once the ratio $t/\lambda$ rises above 0.5 there is always an overlap between rotor and stator teeth, even in the unaligned position, so the unaligned inductance rises rapidly. As is well known, the area enclosed between the aligned and unaligned curves is the change in co-energy, which corresponds to the energy converted to force in a single stroke. From the above it is possible to determine the mean shear force per unit area of airgap as a function of airgap MMF, as follows:

$$\text{instantaneous force } F = \frac{\partial W'}{\partial x} = \partial/\partial x\left[\int_0^{\phi} MMF\, d\phi\right]$$

$$\text{Mean force density} = \frac{1}{\lambda^2 l_a}\int_0^{\lambda} F dx$$

The electric loading can be defined as the RMS MMF per unit periphery of the machine. For simplicity, assume that the current is a constant value for one half of a cycle and zero for the other half. Then

$$\text{electric loading } A = \frac{M\hat{M}F}{\sqrt{2}\lambda}$$

The mean force density variation with electric loading for each value of $t/\lambda$ is shown in Fig. 4. From Fig. 4, peak force density can be seen to occur in the region $0.4 < t/\lambda < 0.5$; this correlates well with earlier work, which has shown that the actual peak is at $t/\lambda = 0.42$ [1, 2].

Consider now an alternative configuration, in which a segmental type of rotor construction is adopted. This is illustrated in Fig. 5, which shows a rectilinear machine in

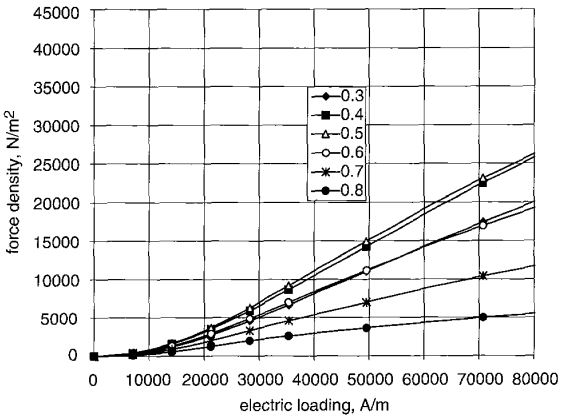


**Fig. 4** *Average airgap force density as a function of RMS electric loading for a doubly salient toothed structure, showing variation with $t/\lambda$*

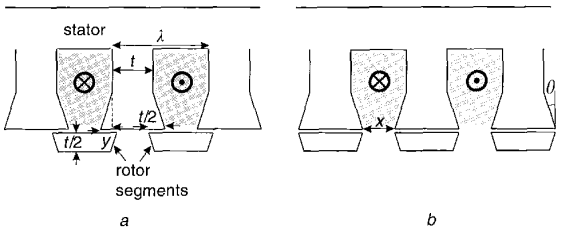


**Fig. 5** *Simple rectilinear model of a doubly salient toothed structure with a segmented rotor*
*a* Aligned position; *b* unaligned position

the same style as the conventional SRM of Fig. 1. (For readers who have problems visualising this machine, a rotating version is discussed later and illustrated in Fig. 15*a*.) The rotor is now a series of lamination segments which, in the aligned position, magnetically shunt a slot. In the unaligned position flux must flow between segments and hence the unaligned permeance is controlled by varying the gap between segments.

The definition of $t$ for this machine is the tooth width in the main body of the tooth, not at the tooth tip. This is consistent with that used in the conventional 'toothed' structure, since in both cases the ratio $t/\lambda$ corresponds to the proportion of the airgap which actively carries magnetic flux at the aligned position. Thus, $t/\lambda$ multiplied by the peak airgap flux density gives a measure of the magnetic utilisation of the structure.

With reference to Fig. 5, the dimensions for the machine are chosen using the following criteria:

(*a*) In the aligned position the length of overlap between each rotor segment and the stator tooth tip is $t/2$, so that the airgap flux density corresponds to the tooth flux density.

(*b*) The vertical height of the rotor segments is equal to one-half of the tooth width, $t$, so that the rotor magnetic flux density is equal to that of the stator.

(*c*) The distance between adjacent rotor segments, $x$, is equal to that between adjacent stator tooth tips: this helps to minimise the unaligned permeance, without compromising the aligned inductance.

Note also that the stator and rotor teeth are tapered at the tips. If the taper angle, $\theta$, is too small the unaligned inductance is unnecessarily increased, whilst if it is too large

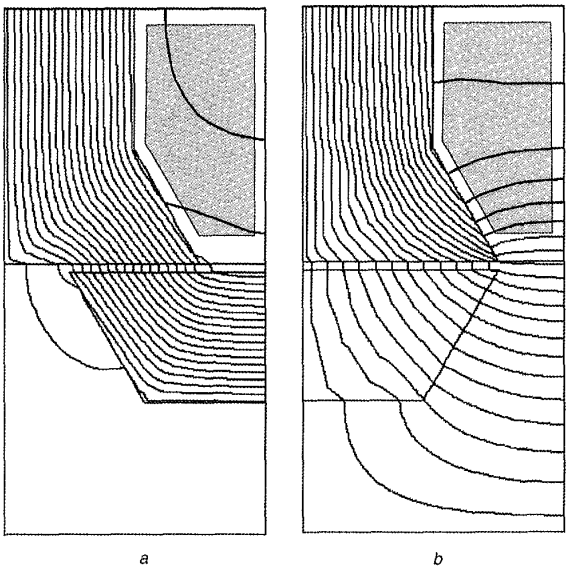


**Fig. 6** *Magnetic flux plots for a doubly salient segmental rotor structure, exploiting symmetry around tooth and slot centre line*
*a* Aligned position; *b* unaligned position

the tooth tip saturates too early, reducing the peak flux density in the aligned position. An angle of 30 degrees was found to give a reasonable compromise in this case.

The segmental structure will now be compared to the toothed structure, maintaining a slot pitch, $\lambda$, of 20.0 mm and an airgap length of 0.3 mm. Fig. 6 shows magnetic flux distribution in the aligned and unaligned position and Fig. 7 shows the flux-linkage per unit length as a function of slot MMF in the segmental machine, once more for a range of values of $t/\lambda$. As might be expected, the aligned flux-linkage for the segmental rotor machine corresponds closely with that of the conventional machine (shown as a dashed line in the figure). However, the unaligned flux-linkage is substantially different. When $t/\lambda < 0.5$ the segmental rotor exhibits a higher unaligned flux linkage, predominantly due to the semi-closed nature of the stator slots, which increases the cross slot flux. However, once $t/\lambda$ increases above 0.5 the opposite occurs, with the segmental design having a lower unaligned flux-linkage. This is because the conventional design has overlapping teeth, even in the unaligned position when $t/\lambda > 0.5$ corresponding to an unacceptably high unaligned permeance, whilst the segmental design always maintains a gap between rotor segments, across which unaligned flux must pass.

Fig. 8 shows the effect on the mean force density. From Fig. 8*b* the two machines can be seen to have a very similar force density when $t/\lambda < 0.4$, but when $t/\lambda > 0.5$ the segmental design offers greatly superior performance. As $t/\lambda$ rises beyond 0.5 in the segmental design the force density continues to rise, even when $t/\lambda$ approaches 0.8. By this time the force density is between 1.6 and 1.8 times greater than that which can be achieved with the best possible conventional toothed design. Of course it is not generally sensible to design a machine with $t/\lambda > 0.5$ because it results in a very narrow slot, with insufficient room for the winding. Hence, unless other gains can be found, the segmental design is no more than an academic novelty, with the magnetic capability of increased torque production but no practical application.

Axially laminated rotor designs offer maximum performance for synchronous reluctance motors, and so it is

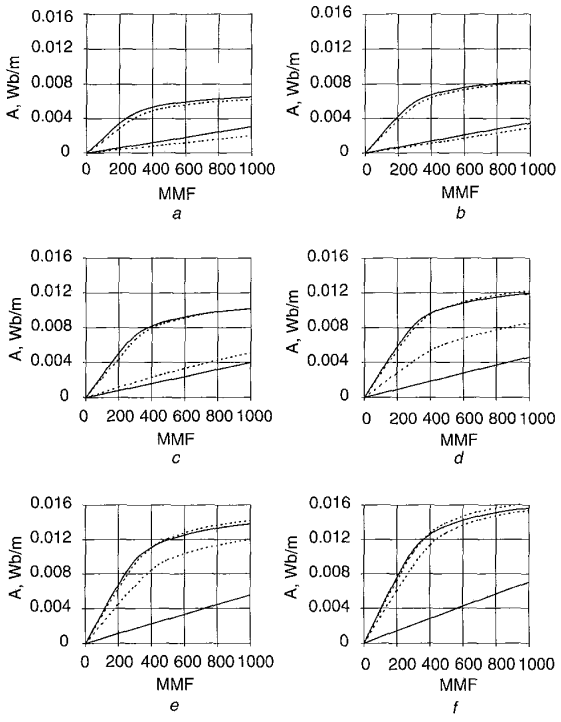


**Fig. 7** *Average magnetic vector potential against MMF per half-slot for a doubly salient toothed structure, showing the variation with $t/\lambda$*
Equivalent curves for a conventional SRM are shown dashed
$t/\lambda$: *a* 0.30; *b* 0.40; *c* 0.50; *d* 0.60; *e* 0.70; *f* 0.80

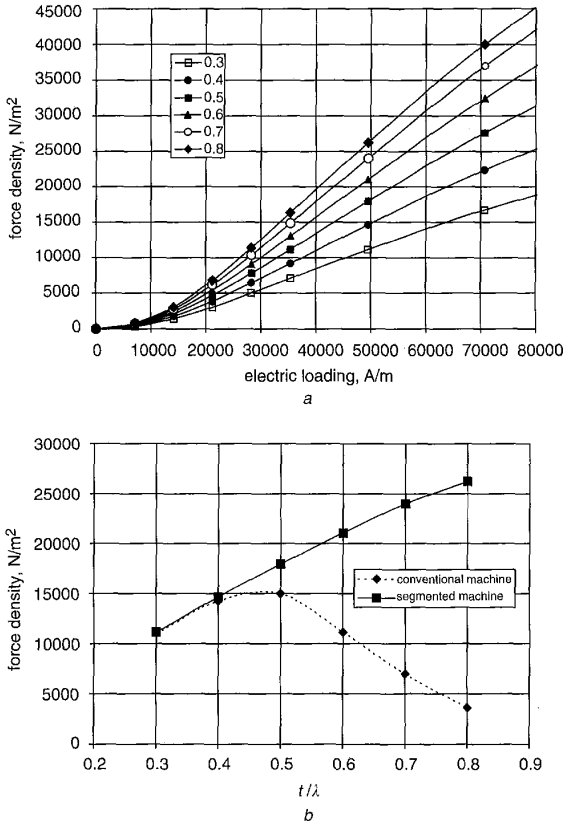


**Fig. 8** *Average airgap force density as a function of RMS electric loading for a doubly salient segmental rotor structure*
*a* Variation with electric loading; *b* variation with $t/\lambda$ for an electric loading of 50 000 $Am^{-1}$

natural to also examine their feasibility in this machine. Xu and Lipo [26–28] have performed extensive work on a two-phase machine of this type, showing very favourable experimental results. Their findings were challenged by Davis [30, 31], who came to the opposite conclusion. For direct comparison with the segmental rotor an axially laminated rotor has been designed with five separate lamination layers. The gaps between each lamination were chosen to be one-half of the lamination thickness. Finite element plots of this design, showing the field distribution in both the aligned and unaligned positions, are shown in Fig. 9, with the stator design identical to that of a segmental design with $t/\lambda = 0.7$. Fig. 9*c* shows the aligned and unaligned flux/MMF curves for this machine, with curves for the segmental rotor shown alongside. In the unaligned position there is a higher flux linkage in the axially laminated design because there is a smaller gap between adjoining rotor poles. This is clearly visible in Fig. 9*b*, where the end rotor lamination carries a substantial field. The aligned flux linkage is lower, simply because there is a smaller rotor iron cross-sectional area. This is inevitable because of the necessity to maintain gaps between the rotor laminations.

The axially laminated design is clearly inferior to the segmental design. With careful optimisation it may be possible to slightly improve the axially laminated design, but it is unlikely to match that of the segmented design. It can be concluded that axially laminated rotors, which distribute the reluctance variation around the rotor, work well with the distributed MMF pattern of a synchronous reluctance motor, but do not offer the best solution for an SRM. With an SRM the MMF is concentrated, and it is better to have a rotor magnetic circuit which has an equally concentrated reluctance, as displayed by the segmental design.

## 3 Direct use of segmental rotor designs in multi-phase machines

The previous section has shown that segmental rotor designs offer advantages over conventional rotor designs in single-phase reluctance motors if $t/\lambda > 0.5$, but the designs are likely to be impractical because there is not enough room for a winding. It must now be asked whether this remains true for multi-phase designs. The remainder of this paper will focus on three-phase designs in which the stator slot pitch, $\lambda_s$, is two-thirds that of the rotor slot pitch, $\lambda_r$.

In conventional, toothed SRMs the rotor and stator core backs form magnetic paths, which can be used to magnetically link poles of equal phase. Thus, for the example of a three-phase structure, as shown in Fig. 10, excitation of like teeth results in the coil MMF shown. Two alternative winding methods may be used to excite these poles: either short pitched, single tooth windings, as shown in Fig. 10, or fully pitched windings. Note that the latter increases electric utilisation of the machine because the whole of the slot either side of a tooth is excited, but requires two phases to be conducting in order to excite a single set of poles.

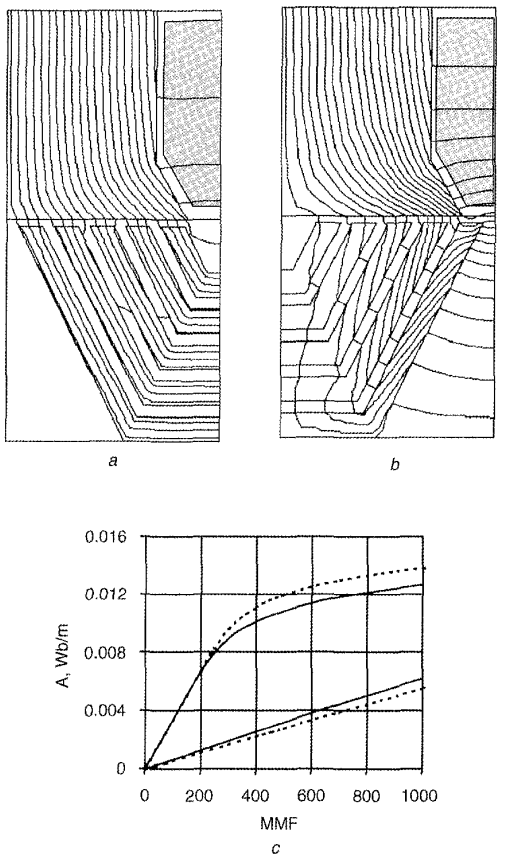


**Fig. 9** *Single-phase machine with axially laminated rotor*
Stator design corresponds to segmental rotor design with $t/\lambda = 0.70$
*a* Magnetic flux plot in aligned position; *b* magnetic flux plot in unaligned position; *c* flux-linkage/MMF diagram (solid lines) with equivalent curves for a segmental rotor shown dashed

With the segmental rotor machine the rotor structure only permits adjoining teeth to be magnetically linked, so the magnetic flux can only enclose a single stator slot. Thus, in moving to a multiphase design it is natural to split the structure so that a single unit comprises one stator slot, and the design should have the capability to excite only those slots of the same phase. The obvious manner in which to do this is to use a winding arrangement where each slot contains only the winding of a single phase. An arrangement which does this is shown in Fig. 11, with each coil spanning three slots.

As in the single-phase design, the gap between rotor segments is chosen to be equal to that of the stator slot opening so that neither the rotor or stator contributes excessively to the unaligned inductance (see Fig. 11). The length of overlap between a rotor segment and the tooth width in the aligned position is also made equal to the main stator tooth width, thus equalising magnetic flux densities throughout the magnetic circuit in the aligned position. From these two design rules the slot opening, $x$, and the tooth tip closure, $y$, can be derived using the following equations:

$$\text{Equating values with the rotor pole arc} \quad t + 2x = \lambda_r \quad (1)$$

$$\text{From the arc of the stator pole} \quad \frac{t}{2} + x + 2y = \lambda_s \quad (2)$$

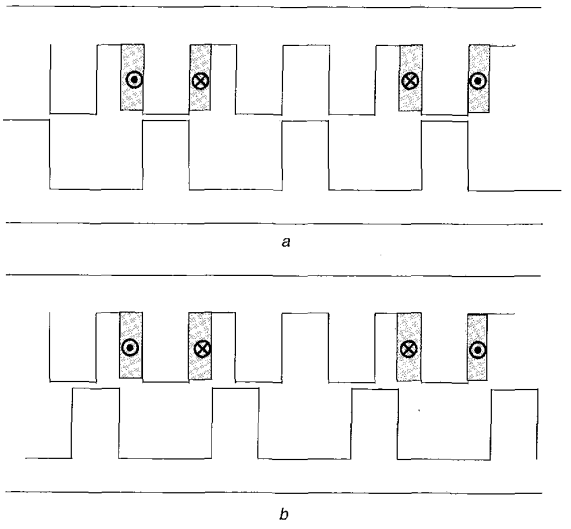


**Fig. 10** *Three-phase toothed rotor design, showing desired MMF pattern of a single phase*
*a* Aligned position; *b* unaligned position

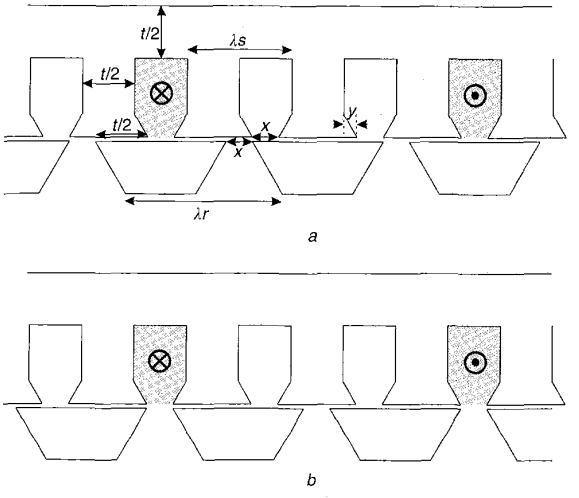


**Fig. 11** *Three-phase segmental rotor design, showing desired MMF pattern of a single phase*
*a* Aligned position; *b* unaligned position

The principal difference between the three-phase and single-phase designs lies in the required width of the stator teeth. In the single-phase version each stator tooth had to carry the flux from two rotor segments, and was of width $t$. In the three-phase version, with one phase excited, each stator tooth carries only the flux of one rotor segment, so the tooth width can be reduced to $t/2$. It is this feature which is critical in making a three-phase segmental rotor SRM a sensible proposition because it allows a high value of $t/\lambda$ whilst retaining enough room for the winding.

Fig. 12 shows the magnetic field distribution for rectilinear representations of three-phase machines; both conventional toothed rotor and segmental rotor constructions are shown with identical stator tooth widths. Whilst in the conventional machine $t/\lambda = 0.33$, in the segmental machine $t/\lambda = 0.67$, so that the segmental machine can carry much more flux, whilst retaining most of the slot area and thus the electric loading capability. Fig. 13 shows the flux/MMF

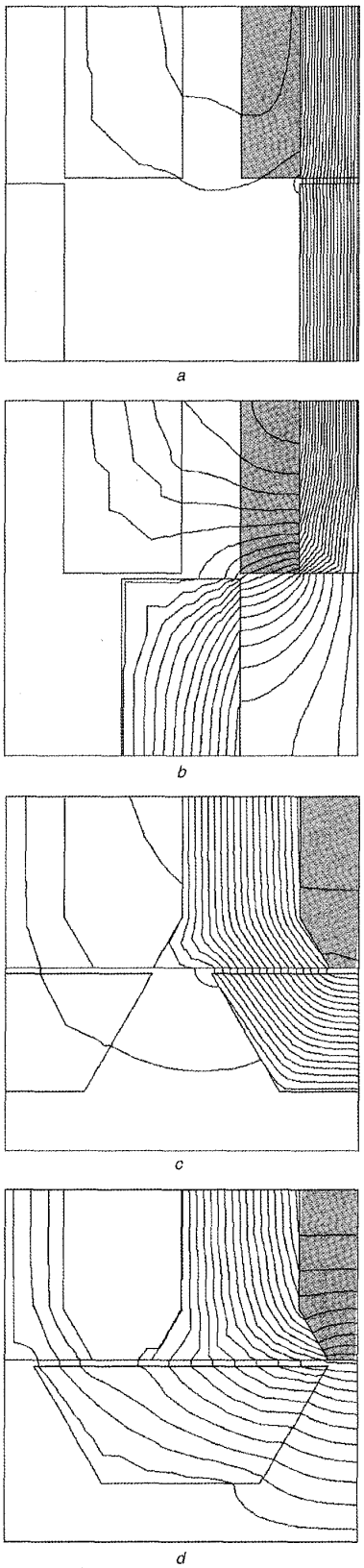


**Fig. 12** *Magnetic flux plots for three-phase machine geometries with equal slot and tooth widths*
*a* Toothed rotor design in aligned position ($t/\lambda = 0.33$); *b* toothed rotor design in unaligned position ($t/\lambda = 0.33$); *c* segmental rotor design in aligned position ($t/\lambda = 0.67$); *d* segmental rotor design in unaligned position ($t/\lambda = 0.67$)

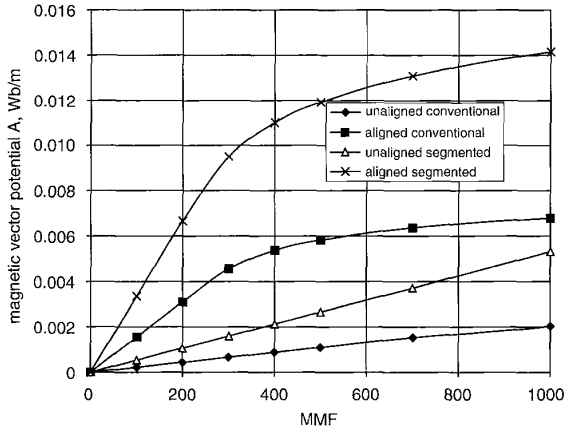


**Fig. 13** *Average magnetic vector potential against MMF per half-slot for both three-phase conventional toothed rotor and segmented rotor structures*
Both machines have equal stator tooth width, corresponding to $t/\lambda = 0.33$ in conventional machine and $t/\lambda = 0.67$ in segmented machine

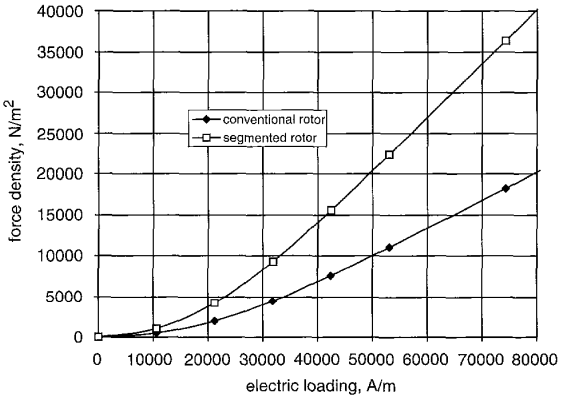


**Fig. 14** *Average airgap force density as a function of RMS electric loading for both three-phase conventional toothed rotor and segmented rotor structures, corresponding to Fig. 12*

diagrams for these machines, and Fig. 14 compares their force density capability as a function of electric loading, showing that the segmental machine has approximately double the torque capability, irrespective of the electric loading. This is a direct result of the segmental machine having twice the flux of the conventional toothed machine.

The above reasoning is not entirely complete. Whilst the conventional, toothed rotor SRM has short pitched windings placed around a single tooth, the segmental SRM has windings which enclose a complete magnetic pole, comprising three teeth, so the winding can be classed as fully pitched. Whilst the winding is identical to that employed in conventional SRMs with fully pitched windings [18], the similarity ends there. In the segmental rotor SRMs, torque results from changing self-inductance, whilst in toothed rotor SRMs with fully pitched windings, the torque is produced by changing mutual inductance, and therefore the latter machine requires two or more phases to be simultaneously conducting.

Compared to a conventional short pitched winding SRM there are considerably longer end-windings, which produce additional copper mass and winding loss. The importance

of this additional loss is dependent on the machine axial length and pole number; this importance will be addressed later.

## 4 Three-phase demonstrator machine

To test the concept of segmental rotor SRMs a rotating machine has been built and tested. The machine is three-phase, with 12 teeth on the stator and 8 rotor segments. As the coils must span three stator teeth this topology requires each end-winding of the machine to span one-quarter of the machine, i.e. it is a four-pole winding. This gives a substantially shorter end-winding than an equivalent 6-4 machine, but is still longer than for a conventional SRM.

To provide direct comparison with other SRMs which have been produced at the University of Newcastle, the machine has been built with an outside diameter of 150 mm and a lamination stack length of the same value. When choosing the ratio of $t/\lambda$ a compromise is required between maximising magnetic flux with a large value of $t/\lambda$ and maximising the electric loading with a large slot width and therefore low $t/\lambda$. For this machine the tooth width and slot width were chosen to be effectively the same, resulting in $t/\lambda = 0.67$.

The rotor segment laminations were mounted on a steel shaft. This shaft was constructed from nonmagnetic steel so that it did not produce a magnetic flux path between rotor segments. The rotor segments required both circumferential location and retention against centripetal and magnetic radial forces when rotating. Circumferential location was achieved by using flat bottoms on the rotor segment laminations, matched into inserts in the shaft (see Fig. 15*a*). Radial retention of the rotor segments was achieved by non magnetic steel wedges, which were dovetailed into protrusions at the bottom of each segment, and then bolted on to the rotor shaft. The bolt heads are visible in the photograph of Fig. 16*a*, which shows the assembled rotor. Fig. 16*a* also

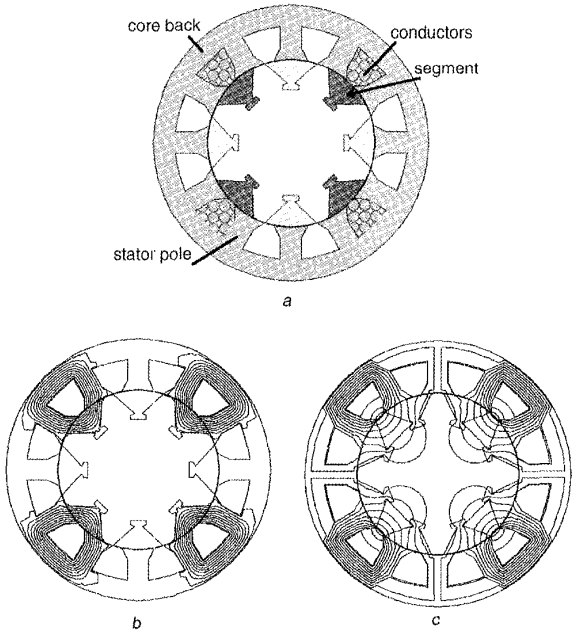


**Fig. 15** *Three-phase prototype machine*
*a* Schematic layout, showing one phase excited in aligned position; *b* magnetic flux plot, showing one phase excited in aligned position; *c* magnetic flux plot, showing one phase excited in unaligned position

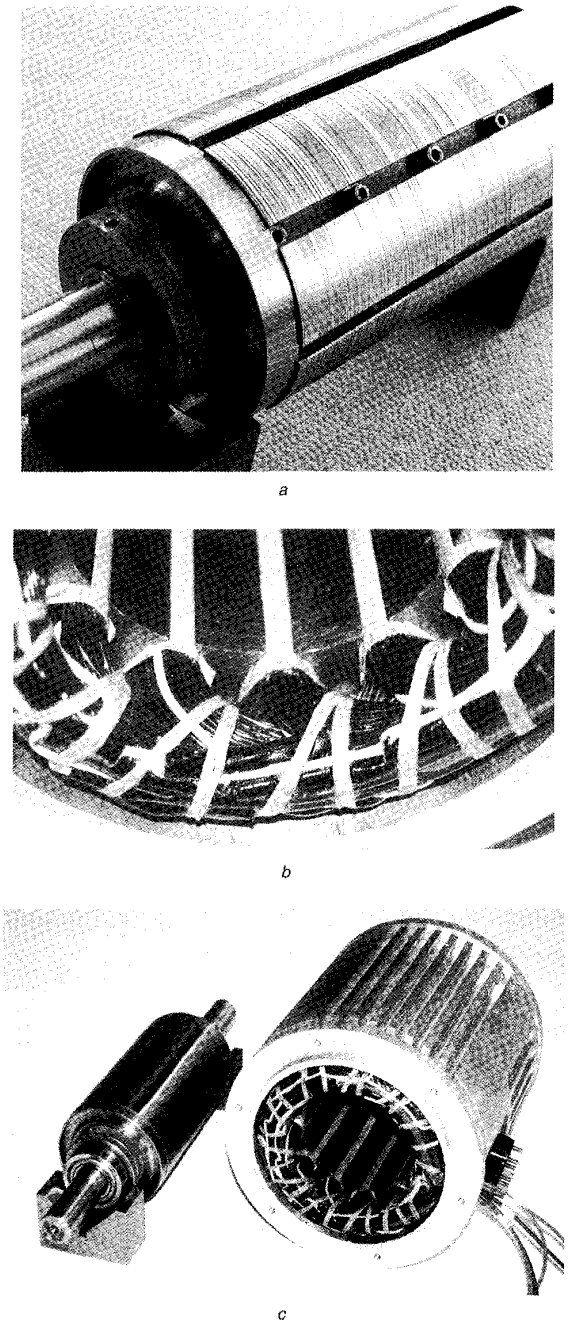


**Fig. 16** *Photographs of three-phase prototype machine*
*a* Rotor, showing segments and retaining wedges before 'potting'; *b* detail of stator end-winding, showing coils linking three teeth; *c* finished rotor and stator before final assembly

shows rotor end-rings, which were used to apply axial pressure on the rotor segment laminations. After assembly the rotor was 'potted' with an epoxy resin, and finally turned in a lathe to its final outside dimension. This arrangement proved very successful, and is designed for a safe working speed of up to 6000 rev/min.

Fig. 16*b* shows in detail the stator end-winding – it is a standard double layer, 'basket' winding, commonly used in AC machines. The end-winding stands out 37mm at each end of the lamination stack, and is therefore significantly longer than in a standard SRM, but certainly no longer than is typical in an induction motor. Finally the completed

**Table 1: Dimensions of the prototype machine and a fully pitched winding toothed rotor SRM, used for comparison**

| | Segmental rotor prototype machine | Toothed rotor SRM |
|---|---|---|
| Number of phases | 3 | 3 |
| Number of stator slots | 12 | 12 |
| Number of rotor segments/teeth | 8 | 8 |
| Outside diameter, mm | 150.0 | 152.6 |
| Stack axial length (rotor and stator), mm | 150.0 | 150.0 |
| Rotor outside diameter, mm | 90.8 | 89.6 |
| Airgap length, mm | 0.3 | 0.25 |
| Stator tooth width, mm | 11.93 (parallel sided) | 12.05 at tip, with 12 degree taper |
| Arc of stator tooth tip, deg. | 22.5 | 15.0 |
| Stator core back depth, mm | 11.9 | 10.6 |
| Arc of rotor segments/teeth, deg | 37.5 | 16.2 |
| Number of series turns/phase | 300 | 204 |
| Coil span | 3 slots (90 mechanical degrees) | 3 slots (90 mechanical degrees) |
| Effective wire diameter, mm | 1.0 | 1.20 |
| Slot fill-factor (copper area to overall slot area), % | 46 | 42 |
| Resistance per phase at 20°C, Ω | 3.58 | 1.825 |

rotor and stator are shown in Fig. 16*c*. The major dimensions of the prototype machine are tabulated in Table 1.

Sample finite element field distributions, showing one phase excited in both the aligned and unaligned position, are given in Fig. 15. Unlike a conventional, short pitched winding SRM there are only the conductors of one phase in a slot, so there is no mutual coupling between phases due to cross-slot leakage, although a very low level of inter-phase coupling is evident via the rotor. It is particularly notable how the core back flux is equal in magnitude to the peak tooth flux (in a conventional SRM it is one-half of this), and hence it is necessary to use a relatively deep core back. This is less of a penalty than first appears; the core back depth in conventional SRMs is often increased beyond that required magnetically in order to increase mechanical stiffness and thereby reduce acoustic noise. Because the machine naturally has short flux loops, only one-third of the core back circumference is used by any one phase, and thus it is reasonable to assume that core back iron loss is reduced by this feature. The gains in core back iron loss are expected to be countered by increased iron loss in the teeth, which must carry the flux of two adjoining phases. This subject will be a topic of further study.

The machine has been subjected to static torque tests, the results of which are displayed in Fig. 17. At high excitation levels the general form of the static torque curves is similar to that of a conventional SRM when the machine is saturated, but differs significantly at low currents. In an unsaturated, conventional SRM the magnetic permeance rises almost linearly with angle of overlap of the teeth, resulting in an almost constant torque during this period. In the segmental machine the permeance does not vary in such a simple manner: as the area of overlap on one side of the

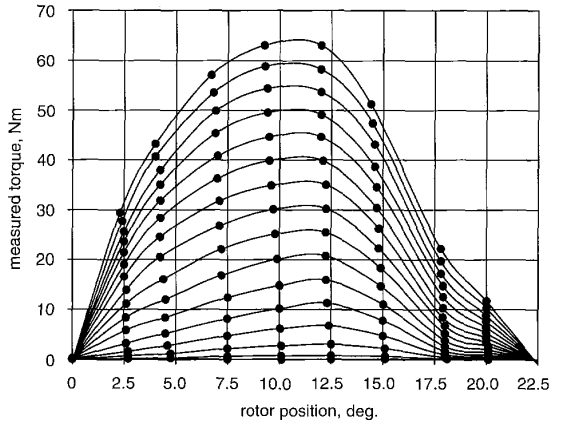


**Fig. 17** *Measured static torque profiles with one phase of the three phase machine excited*
Each curve corresponds to constant current excitation, ranging from 0.0 to 15.0 A in increments of 1.00 A

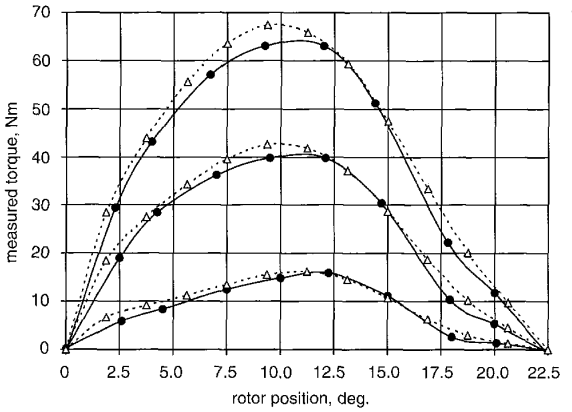


**Fig. 18** *Comparison between measured and predicted static torque curves with one phase of the three phase machine excited*
Measured static torque (solid line) and simulated (dashed line) in steps of 5 A to 15.0 A

magnetic circuit increases, it decreases on the other. This results in a static torque which rises to reach a peak at approximately 12.5 degrees from the aligned position.

Fig. 18 gives a comparison between measured static torques and those predicted using two-dimensional finite element analysis. The comparison is generally good, both in terms of the shape of the curves and their magnitude. The simulation has taken no account of three-dimensional end-effects, and so this comparison is certainly as good as can be expected. At very large currents the discrepancy is larger, when the simulation tends to overestimate the mean torque by a few percent.

Of most importance is the mean torque capability of the machine at thermal limit. The variation of mean torque as a function of total machine winding loss was determined, the loss being found from the measured machine's electrical resistance. This loss estimate assumed that each phase conducted a constant current for one-third of a cycle, with the period of conduction symmetrical about the position of peak torque. The same torque capability estimate was produced for a conventional SRM with short-pitched windings and with a fully pitched winding SRM with a toothed rotor structure. The latter was taken directly from

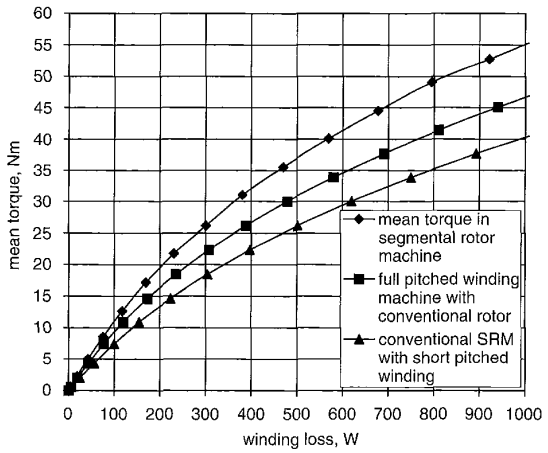


**Fig. 19** *Comparison of mean torque capability as a function of winding loss for three machines under unipolar current control*
Comparisons take into account differing end-winding lengths and excitation periods. Curves for segmental and conventional fully pitched winding machines are by measurement, whilst that for conventional short pitched winding SRM is based on simulation

measurements made on a machine with the same outside diameter and lamination stack length (see Table 1). No measured data were available for the conventional SRM with short-pitched windings, so simulated results are presented instead.

In terms of copper loss the short pitched winding SRM immediately had a major advantage due to its smaller end-windings: this resulted in its having only 65% of the total winding mass. Hence, for a given winding loss, it could operate with $1/\sqrt{0.65} = 1.24$ times greater RMS current density. The machine has the same magnetic geometry as the fully pitched winding machine with a toothed structure, corresponding to $t/\lambda = 0.33$. Fig. 19 shows that if a mean torque of 24Nm is produced a total winding loss of 440 W was incurred.

The fully pitched winding SRM with a toothed rotor has previously been shown to be capable of operating with both unipolar and bipolar currents [18]. Maximum torque capability occurs with bipolar excitation, but this has been found to require a greater converter volt-ampere rating, so is not considered here; only a unipolar excitation sequence is considered. The machine gains over the short-pitched winding SRM because two phases can simultaneously contribute to the MMF per pole, thus increasing the MMF capability of the machine, despite the increased winding length. In comparing machines account is taken of the requirement in one machine to have two phases simultaneously conducting, and the subsequent increase in winding loss. Fig. 19 shows that the fully pitched winding machine has 340 W of winding loss when delivering a mean torque of 24 Nm.

The segmental rotor machine has been shown to offer increased magnetic flux-linkage over the other machines. It has an identical winding pattern and very similar copper mass to the fully pitched machine, but each phase needs to conduct for only one-third of a cycle. It can deliver 24 Nm of torque with only 260 W of loss, which is well within the steady-state thermal capability of the machine.

If the three machines are viewed in terms of torque capability for a given loss, then for 300 W of winding loss, which corresponds to ~100 degrees centigrade rise without forced ventilation, the conventional SRM can deliver 18.4 Nm, the toothed SRM with fully pitched windings can deliver 22.0 Nm, and the new segmental machine 26.1 Nm. Fig. 19 shows how these gains are apparent over a wide range of winding loss values.

It is interesting to note theoretically that, even if the conventional SRM with short-pitched windings could have the amount of copper in its slots increased until it had the same volume of copper in total as the other two machines, it would still give a few percent less torque than the segmental rotor SRM. (This would require the slot to be 71% full of copper!)

## 5 Conclusions

A segmental rotor construction can be used to increase the performance of switched reluctance motors, also offering gains over axially laminated rotor designs. In single-phase machines the airgap force density exceeds that of a conventional SRM when the active portion of the airgap exceeds one-half of a pole pitch. However, under such circumstances there may be insufficient room for the windings. In three-phase machines the airgap force density has been calculated as a function of electric loading and shown to be almost exactly double that of a conventional SRM. The principal reason for the increase in performance is due to better magnetic utilisation of the machine, which has double the active airgap area of a conventional SRM. However, the segmental designs presented require a fully pitched winding, which increases the copper mass and end-winding losses.

A three-phase, segmental rotor SRM has been built and tested. Torque has been measured as a function of both current and position, showing good agreement with predictions. Comparisons with other switched reluctance machines of the same outside diameter and core length have shown a 41% increase in torque per unit copper loss at thermal limit. The increased end-winding length requires more copper and so the torque per unit copper mass is not increased.

## 6 References


1 HARRIS, M.R., HUGHES, A., and LAWRENSON, P.J.: 'Static torque production in saturated doubly-salient machines', *Proc. IEE*, 1975, **122**, (10), pp. 1121–1127
2 HARRIS, M.R., ANDJARGHOLI, V., LAWRENSON, P.J., HUGHES, A., and ERTAN, B.: 'Unifying approach to the static torque of stepping-motor structures', *Proc IEE*, 1977, **124**, (12), pp. 1215–1224
3 LAWRENSON, P.J., STEPHENSON, J.M., BLENKINSOP, P.T., CORDA, J., and FULTON, N.N.: 'Variable-speed switched reluctance motors', *IEE Proc. B*, 1980, **127**, (4), pp. 253–265
4 MILLER, T.J.E.: 'Switched reluctance motors and their control', (Clarendon Press, Oxford, 1993)
5 NEAGOE, C., FOGGIA, A., and KRISHNAN, R.: 'Impact of pole tapering on the electromagnetic torque of the switched reluctance motor'. 1997 IEEE International electric machines and drives conference record, WA1/2.1-3, Milwaukee, WI, USA, 18–21 May 1997
6 WU, C., and POLLOCK, C.: 'Analysis and reduction of vibration and acoustic noise in the switched reluctance drive', *IEEE Trans. Ind. Appl.*, 1995, **31**, (1), pp. 91–98
7 SANADA, M., MORIMOTO, S., TAKEDA, Y., and MATSUI, N.: 'Novel rotor pole design of switched reluctance motors to reduce the acoustic noise', IEEE Conference on industry applications, Rome, October 2000
8 PILLAY, P., and CAI, W.: 'An investigation into vibration in switched reluctance motors', IEEE Trans. Ind. Appl., 1999, **35**, (3), pp. 589–597
9 LOVATT, H.C., and STEPHENSON, J.M.: 'Influence of number of poles per phase in switched reluctance motors', *IEE Proc. B*, 1992, **137**, (4), pp. 307–314
10 WALLACE, R.S., and TAYLOR, D.G.: 'Three phase switched reluctance motor design to reduce torque ripple', International conference on electrical machines *ICEM'90*, Boston, pp. 782–787
11 EASTHAM, A.R., YUAN, H., DAWSON, G.E., CHOUDHURY, P.C., and CUSACK, P.M.: 'A finite element evaluation of pole shaping in switched reluctance motors', *Electrosoft*, 1990, **1**, (1), pp. 55–67

12 SAHIN, F., ERTAN, B., and LEBLEBICIOGLU, K.: ' Optimum geometry for torque ripple minimisation of switched reluctance motors'. International Conference on Electrical Machines ICEM' 96, Vigo, Spain, Vol. **2**, pp. 110–115
13 HOANG, E., MULTON, B., VIVES FOS, R., and GEOFFROY, M.: 'Influence of stator yoke thickness and stator teeth shape upon ripple and average torque of switched reluctance motors', SPEEDAM Conf., Taormina, Italy, 8–10 June 1994, pp. 145–149
14 FINCH, J.W., HARRIS, M.R., MUSOKE, A., and METWALLY, H.M.B.: 'Variable speed drives using multi-tooth per pole switched reluctance motors', *Increm. Motion Control Syst. Devices News.*, 1984, **13**, pp. 293–301
15 FINCH, J.W., HARRIS, M.R., METWALLY, H.M.B., and MUSOKE, A.: 'Switched reluctance motors with multiple teeth per pole: philosophy of design', Proc. IEE Conference on electrical machines-design and application, London, Sept. 1985, pp. 134–138
16 LINDSAY, J.F., ARUMUGAM, R., and KRISHNAN, R.: 'Finite element analysis of a switched reluctance motor with multitooth per stator pole', *IEE Proc. B*, 1986, **133**, (6), pp. 347–353
17 MECROW, B.C.: 'Fully pitched-winding switched reluctance and stepping-motor arrangements', *IEE Proc. B*, 1993, **140**, (1), pp. 61–70
18 MECROW, B.C.: 'New winding configurations for doubly salient reluctance machines', *IEEE Trans. Ind. Appl.*, 1996, **32**, (6), pp. 1348–1357
19 LIANG, F., and LIPO, T.A.: 'New variable reluctance motor utilising an auxiliary commutation winding', *IEEE Trans., Ind. Appl.*, 1994, **30**, (2), pp. 423–432
20 LAWRENSON, P.J., and AGU, L.A.: 'Theory and performance of polyphase reluctance machine', *Proc. IEE*, 1964, **111**, (8), pp. 1435–1445
21 LAWRENSON, P.J., and GUPTA, S.K.: 'Developments in the performance and theory of segmental-rotor reluctance machines', *Proc. IEE*, 1967, **114**, (5), pp. 645–653
22 MILLER, T.J.E., HUTTON, A., COSSAR, C., and STATON, D.A.: 'Design of a synchronous reluctance motor drive', *IEEE Trans., Ind. Appl.*, 1991, **27**, (4), pp. 741–749
23 VAGATI, A., FRANCESCHINI, G., MARONGIU, I., and TROGLIA, G.P.: 'Design criteria for high performance synchronous reluctance motors', *IEEE* IAS Annual Meeting Record, 1992, pp. 66–73
24 CRUICSHANK, A.J.O., MENZIES, R.W., and ANDERSON, A.F.: 'Axially laminated anistropic rotor for reluctance motors', *Proc. IEE*, 1966, **113**, (12), pp. 2058–2060
25 CRUICSHANK, A.J.O., MENZIES, R.W., and ANDERSON, A.F.: 'Theory and performance of reluctance motors with axially laminated rotors', *Proc. IEE*, 1971, **118**, (7), pp. 887–894
26 LONGYA, XU, LIPO, T.A., and RAO, S.C.: 'Analysis of a new variable-speed singly salient reluctance motor utilizing only two transistor switches', *IEEE Trans., Ind. Appl.*, 1990, **26**, (2), pp. 229–236
27 LONGYA, XU: 'Design and evaluation of a converter optimised synchronous reluctance motor drive'. PhD thesis, University of Wisconsin-Madison, 1990
28 LIPO, T.A. and LONGYA, XU: 'Variable speed machine with high power density'. United States Patent No. 5,010,267,' 23 April 1991
29 HORST, G.A.: 'Isolated segmental switched reluctance motor'. United States Patent No. 5,111,096,' 5 May 1992
30 DAVIS, R.M.: 'A comparison of switched reluctance rotor structures', *IEEE Trans., Ind. Electron.*, 1988, **35**, (4), pp. 524–529
31 DAVIS, R.M.: 'Variable reluctance rotor structures – their influence on torque production', *IEEE Trans., Ind. Electron.*, 1992, **39**, (2), pp. 168–174